JOURNAL OF VIROLOGY, Jan. 2010, p. 503–515 Vol. 84, No. 1
0022-538X/10/$12.00 doi:10.1128/JVI.01134-09

Targeting of Murine Leukemia Virus Gag to the Plasma Membrane Is Mediated by PI(4,5)P_2/PS and a Polybasic Region in the Matrix▽

E. Hamard-Peron,[1] F. Juillard,[1] J. S. Saad,[2]† C. Roy,[3] P. Roingeard,[4] M. F. Summers,[2] J.-L. Darlix,[1] C. Picart,[3]‡ and D. Muriaux[1]*

LaboRetro, InsermU758, ENS de Lyon, IFR128, 69364 Lyon, France[1]; Howard Hughes Medical Institute and Department of Chemistry and Biochemistry, University of Maryland Baltimore County, 1000 Hilltop Circle, Baltimore, Maryland 21250[2]; CNRS-UMR 5235, Université de Montpellier 2, Montpellier, France[3]; and Inserm U966, Université François Rabelais, Tours, France[4]

Received 3 June 2009/Accepted 1 October 2009

Membrane targeting of the human immunodeficiency virus Gag proteins is dependent on phosphatidylinositol-(4,5)-bisphosphate [PI(4,5)P_2] located in the plasma membrane. In order to determine if evolutionarily distant retroviral Gag proteins are targeted by a similar mechanism, we generated mutants of the matrix (MA) domain of murine leukemia virus (MuLV) Gag, examined their binding to membrane models in vitro, and analyzed their phenotypes in cell culture. In vitro, we showed that MA bound all the phosphatidylinositol phosphates with significant affinity but displayed a strong specificity for PI(4,5)P_2 only if enhanced by phosphatidylserine. Mutations in the polybasic region in MA dramatically reduced this affinity. In cells, virus production was strongly impaired by PI(4,5)P_2 depletion under conditions of 5ptaseIV overexpression, and mutations in the MA polybasic region altered Gag localization, membrane binding, and virion production. Our results suggest that the N-terminal polybasic cluster of MA is essential for Gag targeting to the plasma membrane. The binding of the MA domain to PI(4,5)P_2 appears to be a conserved feature among retroviruses despite the fact that the MuLV-MA domain is structurally different from that of human immunodeficiency virus types 1 and 2 and lacks a readily identifiable PI(4,5)P_2 binding cleft.

Retroviruses are a large family of enveloped viruses that contain two copies of a positive-strand RNA genome. The retroviral replication cycle is canonically divided into early and late stages. The early stage corresponds to virus infection and entry into the target cell, reverse transcription of the genome, and proviral DNA integration into the host cell genome. During the late stage, the integrated provirus is transcribed, generating unspliced and spliced viral RNAs that are translated by the host ribosome machinery. All replicating retroviruses encode three major structural proteins and enzymes, namely, Gag, Pol, and Env, that assemble to form new virions. Much of the current understanding of retroviral replication has been derived from studies of murine leukemia virus (MuLV), a simple gammaretrovirus with a full-length primary transcript that encodes four polyproteins: Pr65Gag, Pr180Gag-Pol, Pr75glyco-Gag, and Pr190glyco-Gag-Pol (13) (the Pol domain contains protease [PR], reverse transcriptase [RT] proteins, and integrase [IN]). Gag, the main retroviral structural protein, consists of several domains, with three of them being functionally conserved among retroviruses: the nucleocapsid (NC) domain, which selects the genomic RNA (17, 34); the capsid (CA) domain, which forms the internal capsid structure of the virus; and the myristoylated matrix (MA) domain, which targets Gag to cellular membranes (24, 44). MuLV Gag also contains a long polypeptide called p12 that connects the MA and CA domains and is involved in recruiting cellular cofactors important for budding (59). The Gag polyprotein multimerizes, the assembly process occurs, and Gag is then cleaved into these individual domains by the viral PR during the particle maturation process concomitant with budding (43).

A number of recent studies have focused on identifying the mechanism by which retroviral Gag proteins are targeted to specific virus assembly sites. Although a large fraction of Gag assembles and buds from the plasma membrane, there is not uniform agreement regarding the path(s) that Gag follows to reach the assembly sites. Newly synthesized Gag proteins may be targeted directly to the plasma membrane (54), or they may indirectly traffic via endosomes (3). MuLV budding can occur in intracellular compartments similar or identical in nature to late endosomes/multivesicular bodies (27, 51), but the importance of this pathway in virus egress was recently questioned (9), as MuLV spreading was not significantly impaired in transgenic mice with defects in multivesicular body biogenesis and trafficking.

Gag trafficking may be driven, at least in part, by the ability of the MA domain to interact with host protein and membranes. Some studies indicated that the MuLV MA domain can be engaged in interactions with cellular proteins directly involved in vesicular trafficking, such as AP-1 (6) or Cav-1 (58), or in cytoskeleton regulation, such as IQGAP-1 (31). In addition, a recent study suggests that there is a preferential budding of MuLV at sites of cell-to-cell contact due to the long cytoplasmic tail of Env (28). However, another element important

* Corresponding author. Mailing address: LaboRetro, Inserm U758, ENS de Lyon, IFR128, 69364 Lyon, France. Phone: 33 4 72 72 86 25. Fax: 33 4 72 72 81 37. E-mail: dmuriaux@ens-lyon.fr.

† Present address: Department of Microbiology, University of Alabama at Birmingham, 845 19th Street South, Birmingham, AL 35294.

‡ Present address: CNRS-UMR 5628, LMGP, 3 Parvis L. Neel, 38016 Grenoble, France.

▽ Published ahead of print on 14 October 2009.

for Gag trafficking and virus assembly is the ability of MA to bind cellular membranes of specific compositions.

In fact, the conserved myristoylation of MA is necessary for Gag anchoring into membranes and infectious particle production for different retroviruses such as MuLV (44) and human immunodeficiency virus type 1 (HIV-1) (20, 56). As shown previously for HIV-1 (60, 62) or Rous sarcoma virus (RSV) (16), membrane binding also requires a polybasic region, which is highly conserved among retroviruses. This region is thought to interact with the negatively charged heads of the cellular membrane phospholipids (36, 62). A previous study (52) showed that mutating this region of Moloney MuLV (MoMuLV) MA impairs viral production and Gag localization, but there is as yet no further functional study. Basic residues could reinforce MA interactions with membranes via electrostatic interactions with the acidic lipids of the membrane, as in the case of RSV (16). For several retroviruses, specific membrane binding has been shown to be mediated by cellular lipids. In particular, phosphatidylinositol-(4,5)-bisphosphate [PI(4,5)P_2] was recently shown to mediate plasma membrane binding by HIV-1 and -2 (12, 39, 48) and equine infectious anemia virus (EIAV) (11). PI(4,5)P_2 plays an important role in cellular trafficking, similarly to all members of the phosphatidylinositol phosphate (PIP) family (see references 19, 29, and 30 for reviews). The PIPs are membrane phospholipids, phosphorylated derivatives of phosphatidylinositol. Their inositol ring can be phosphorylated at three positions (positions 3, 4, and 5), and all combinations of mono-, bi-, or triphosphates are present in cells. They are involved in membrane dynamics and trafficking and play essential roles in major cellular signalization pathways. The synthesis, localization, and degradation of PIPs are highly regulated (30): the location of specific kinases and phosphatases can modify the number and the position of the inositol phosphorylations. Therefore, potential interactions of the PIPs with retroviral MA might determine on which cell membrane Gag is targeted for viral assembly.

HIV-1 Gag membrane binding requires a "myristyl switch," i.e., a conformational change during which the N-terminal myristoylation of Gag, initially sequestered in the MA, becomes exposed and is able to interact with membrane phospholipids (25, 40, 45, 47, 48, 53, 55, 61). Recent structural studies of HIV-1 and -2 suggest that the binding of PI(4,5)P_2 to a conserved cleft triggers this allosteric conformational change that exposes the myristyl group (48, 49). The MuLV MA protein does not contain an obvious PIP binding site, and poor solubility has thus far precluded high-resolution structural studies of the myristoylated MuLV MA protein. It is possible, however, to replace HIV MA with MuLV MA with limited effects on viral replication, suggesting a conserved function for this domain among retroviruses (10, 42). To determine if this evolutionarily distant retrovirus uses a similar PIP-dependent mechanism for membrane targeting of the Gag polyprotein, we prepared and characterized native and mutant forms of MuLV MA mutants. In doing so, we discovered an unusual lipid binding mode that appears to depend on both PI(4,5)P_2 and phosphatidylserine.

MATERIALS AND METHODS

Plasmids and site-directed mutagenesis. Plasmids used were pRR88 expressing MoMuLV (35) and pFMLV-Y1 (pY1), which contains the *gag-pol* gene of Friend MuLV (FrMuLV) (57). Substitution mutations were made in the MA coding region in pY1 by using the QuikChange mutagenesis kit (Stratagene), according to the manufacturer's protocol, as shown in Fig. 4. The first mutant series, m1 to m3, are substitutions in the polybasic region of MA. Mutant m1 harbors a replacement of basic arginines 31, 33, and 34 by glycines, mutant m2 harbors a replacement of basic residues R31 to R33 by alanines, and mutant m3 harbors a replacement of basic arginines R31 and R33 by glutamic acids to neutralize charges of the basic K32 and R34 residues. The second mutant series, m4 to m6, are replacements of single basic arginines in MA by glycines. The primers used for mutagenesis are as follows (5′ to 3′): CTGTCGGTAGAGGT TGGAAAAGGGGGCTGGGTTACATTC for m1, CTGTCGGTAGAGGTTG GAGGAGGGCGCTGGGTTACATTCTGC for m2, CTGTCGGTAGAGGTT GAAAAAGAGCGCTGGGTTACATTCTGC for m3, TGGAGGGATGTCGA AGGGACAGCCCACAACCTG for m4, AACGTCGGATGGCCAGGAGAC GGCACTTTTA for m5, GACCCCCCTCCCTGGGTCGGACCCTTCGT GCAC for m6, and the corresponding reverse primers. Plasmid pMyr(−) (2) codes for the unmyristylated protein G2A-Gag-Pol. Plasmid phCMV-MLV-EnvA (50) codes for the envelope glycoprotein derived from amphotropic MuLV strain 4070A. Plasmid pMLV-VL30-GFP (Transgene SA) allows the expression of the MLV-VL30-Psi RNA coding for the green fluorescent protein (GFP) reporter. Plasmid PCS2-Venus, a kind gift from A. Miyawaki, encodes yellow fluorescent protein (YFP) under the cytomegalovirus promoter. The His_6-tagged MuLV unmyristoylated MA [myr(−)MA] plasmid (pET16b-MA) was constructed by ligating the MA coding sequence, which was PCR amplified from the pNCA isolate (NCBI accession number NC_001501), into *Escherichia coli* expression vector pET16b at BamHI and NcoI sites in frame with the C-terminal His_6 tag and stop codon of the plasmid. The plasmid was verified by sequencing at the W. M. Keck Foundation Biotechnology Resource Laboratory at Yale University (New Haven, CT). Substitution mutations were made in the MA coding region in pET-16b-MA using the QuikChange mutagenesis kit (Stratagene) according to the manufacturer's protocol, as shown in Fig. 2. The mutations are the same as the first group of mutants described above except that the primers used for the mutagenesis are adapted to an MoMuLV strain and are as follows (5′ to 3′): CAGTCGGTAGATGTTGGAAAAGGGGGCTGGGTTAC CTTC for m1, CAGTCGGTAGATGTTGGAGGAGGGAGATGGGTTACCT TCTGC for m2, CAGTCGGTTGATGTTGAAAAAGAGCGCTGGGTTACC TTCTGC for m3, and the corresponding reverse primers.

The plasmids expressing 5PhosphataseIV (pcDNA4TOMyc5ptaseIV and the Δ1 mutant) were a kind gift of Eric Freed (HIVDRP, NCI—Frederick) (as described in reference 39). The plasmid expressing the plextrin homology (PH) domain of phospholipase C fused to cyan fluorescent protein (CFP) (pPH-PLC-CFP) was a kind gift of Walter Mothes (Section of Microbial Pathogenesis, Yale University School of Medicine).

Production of recombinant MA. Wild-type MuLV-MA protein, purified under native conditions, was overexpressed in *E. coli* cells (BL21 Codon Plus RIL) by the transformation of plasmid pET16b-MA. Cells were grown at 37°C in LB medium until the optical density at 600 nm reached 0.6 to 0.7 and were then induced with 1 mM isopropyl-D-thiogalactoside (IPTG) for 4 h. Cells were then spun down, and the pellet was lysed using a microfluidizer in a buffer containing 50 mM sodium phosphate, 500 mM sodium chloride, 5 mM β-mercaptoethanol, and 5 mM methionine. The MuLV myr(−)MA protein was purified by cobalt affinity chromatography (Clontech, Mountain View, CA) and ion-exchange column chromatography (SP column). Molecular weight was confirmed by electrospray ionization mass spectrometry. The MuLV myr(−)MA protein was then stored in a buffer containing 50 mM sodium phosphate, 100 mM NaCl, and 5 mM dithiothreitol.

Mutants and wild-type MA proteins, purified under denaturing conditions, were overexpressed in *E. coli* cells (BL21 Codon Plus RIL). Cells were grown at 30°C in LB medium until the optical density at 600 nm reached 0.6 to 0.7 and were the induced with 0.5 mM IPTG overnight. Cells were then spun down, and the pellet was lysed by sonication in a buffer containing 6 M guanidinium, 0.1 M NaH_2PO_4, 0.01 M Tris, 10% ethyl alcohol, 10 mM imidazole, 500 mM NaCl, and 10 mM β-mercaptoethanol (pH 7). The unmyristylated wild-type and mutant MA proteins were purified by nickel affinity chromatography (Ni-nitrilotriacetic acid spin columns; Invitrogen). Elution was done by using a buffer containing 6 M guanidinium, 0.1 M NaH_2PO_4, and 0.01 M Tris (pH 4.5). A 48-h dialysis was performed against KCl-HEPES buffer (100 mM KCl, 0.5 mM EGTA, 20 mM HEPES [pH 7.4]). Aggregated proteins were removed by centrifugation (20 min at 13,000 rpm).

Reagents. 1-Palmitoyl-2-oleoyl-*sn*-glycero-3-phosphatidylcholine (PC) and 1-palmitoyl-2-oleoyl-*sn*-glycero-3-phosphatidylserine (PS) were obtained from Avanti Polar Lipids (Alabaster, AL). The ammonium salt of PI(4,5)P_2 was purchased from Lipid Products (Surrey, Great Britain). D-*myo*-Phosphati-

dylinositol-3-phosphate [PI(3)P], D-*myo*-phosphatidylinositol-4-phosphate [PI(4)P], D-*myo*-phosphatidylinositol-5-phosphate [PI(5)P], D-*myo*-phosphatidylinositol-3,4-bisphosphate [PI(3,4)P_2], D-*myo*-phosphatidylinositol-3,5-bisphosphate [PI(3,5)P_2], and D-*myo*-phosphatidylinositol-3,4,5-triphosphate [PI(3,4,5)P_3] were purchased from Echelon Bioscience (Tebu-Bio, France).

Quantitative cosedimentation assay with LUVs. MA affinity for phospholipids was determined by sedimentation assays with sucrose-loaded large unilamellar vesicles (LUVs) as previously described (4). We incubated a constant amount (1 μM) of recombinant MA protein (see the purification protocol described above) with different concentrations of LUVs, from 1.5 mg/ml to 15.625 μg/ml of total accessible lipids in KCl-HEPES buffer (100 mM KCl, 0.5 mM EGTA, 20 mM HEPES [pH 7.4]) for 10 min at room temperature. The 100-μl samples were then centrifuged (30 min at 42,200 rpm in a Beckman 42.2 Ti rotor). The top 90 μl of each sample was removed and considered the supernatant, and the pellet was resuspended by the addition of 80 μl of KCl-HEPES buffer. The supernatant and pellet were analyzed on a 15% sodium dodecyl sulfate (SDS)-polyacrylamide gel electrophoresis (PAGE) gel, transferred onto Immobilon-P (Millipore) membranes, and stained with Coomassie blue for quantification (4). Since 10 μl of the supernatant was counted as pellet, and since the supernatant and pellet resuspension volumes were identical, the true pellet intensity was calculated using the following formula: $I_{\text{Pellet}} = I_P - 0.1\ I_{SN}$, where I_P and I_{SN} are the experimental intensity values of the pellet and supernatant, respectively. The corresponding percentage of MA bound was deduced [the percentage of MA bound is $I_{\text{Pellet}}/(I_P + I_{SN})$]. The binding of the protein to lipid bilayers can be described by defining an apparent association constant, K, as described previously (7). K is the proportionality constant between the fraction of proteins bound to the lipids, $[MA]_B$, and the total protein concentration in the aqueous phase, $[MA]_F$.

The fraction of MA bound is given by equation 1:

$$\frac{[\text{MA}]_B}{[\text{MA}]_T} = \frac{K[\text{lipid}]_{ACC}}{1 + K[\text{lipid}]_{ACC}} \quad (1)$$

where $[\text{MA}]_T$ is total MA, and $[\text{lipid}]_{ACC}$ is the accessible lipid concentration. It is assumed here that all the lipids of the outer leaflet of the LUVs are accessible. The association constant, K, deduced from the above-described equation is the reciprocal of the apparent dissociation constant, which is often called the affinity constant, K_d. All the calculated K_d values are given in Table 1.

The composition of the LUVs indicated in Results is expressed in weight percentages. LUVs were composed of PC (neutral) and PIPs (acid) and/or PS (acidic), as indicated in Results.

Cell culture. Human 293T cells and mouse NIH 3T3 cells used in this study were maintained, as described previously (34), in Dulbecco's modified Eagle medium supplemented with 10% fetal calf serum and antibiotics (penicillin-streptomycin).

Antibodies. The polyclonal antibody against MuLV CAp30 used is a purified rabbit antiserum raised against the capsid domain of the MuLV-Gag protein (kind gift from A. Rein, NCI), used at a dilution of 1/5,000. Another anti-CAp30 rabbit antibody was produced by Invitrogen and was used at a dilution of 1/700. A goat antiserum against MuLV-Env gp70 (Quality Biotech) was used at a dilution of 1/2,000. The following monoclonal antibodies were purchased from Santa Cruz: anti-Lamp2 (mouse) (dilution of 1/400) anti-human S6 (mouse) (1/1,000 dilution), and anti-human alpha/beta actin (mouse) (1/200 dilution).

Anti-mouse and anti-rabbit antibodies coupled to horseradish peroxidase (Dako) were used at a dilution of 1/2,000. Anti-mouse antibody coupled to Alexa546 and anti-rabbit antibody coupled to Alexa488 (Molecular Probes, Invitrogen) were used at a dilution of 1/2,000.

Viral protein expression in cells. Viral protein expression was obtained by the transfection of MuLV Gag-Pol expression vectors in 293T and NIH 3T3 cell lines. Transfection was performed by use of the calcium phosphate precipitate method on 293T cells (as described in reference 35) and by use of Lipofectamine coupled to Plus reagent (Invitrogen) on NIH 3T3 cells, according to the manufacturer's instructions. Briefly, cells were plated at a density of 40,000 cells per cm^2 and transfected the day after with 100 ng of DNA per cm^2. This protocol was used for viral production characterization, electron microscopy analysis, and membrane flotation assays. For nonreplicative retroviral vector production, 100 ng of Gag-Pol expression vector, 33 ng of phCMV-MLV-A (Env) vector, and 33 ng of p-Psi-GFP per cm^2 were transfected in 293T cells. For confocal microscopy, 16,000 cells per cm^2 were plated and transfected the day after with 70 ng per cm^2 of Gag-Pol expression vector. For viral expression in the presence of 5PtaseIV, 50 ng of pY1 together with 40 ng of phosphatase or pCS2-Venus vector per cm^2 were cotransfected.

Viral particle purification and immunoblotting. To monitor viral particle production, culture medium containing virus-like particles or retroviral vectors was harvested 24 or 48 h posttransfection. After filtration (0.45 μm), the culture medium was centrifuged on a cushion of 25% sucrose in TNE buffer (10 mM Tris-HCl [pH 7.4], 100 mM NaCl, 1 mM EDTA), at 28,000 rpm for 1 h 15 min in a Beckman SW 32 rotor. The pellet was resuspended overnight at 4°C in TNE buffer and stored at −80°C. To analyze intracellular viral protein content, cells were lysed in radioimmunoprecipitation assay buffer (150 mM NaCl, 20 mM Tris-HCl [pH 8], 1% NP-40, 0.1% SDS, 0.2 mM EDTA) and sonicated. The cell lysate was then clarified for 10 min at 13,000 rpm and tested by the Bradford assay (4a). For Western blot analysis, the purified culture medium (equivalent of 430 μl) and cell lysate (50 μg of total proteins) or 28 μl from membrane flotation assay fractions was mixed into the loading buffer. The proteins were separated onto an SDS–10% PAGE gel and transferred onto a polyvinylidene difluoride membrane, and immunoblotting was performed by using the corresponding antibodies. Secondary antibodies were revealed by using the SuperSignal West Pico substrate (Thermo Scientific).

Viral titer measurement and reverse transcription assay. To measure viral titers, serial dilutions of clarified culture supernatants containing the nonreplicative retroviral vectors (made of MLV Gag, Env, and Psi RNA-GFP) were applied onto NIH 3T3 cells, and the number of cells expressing GFP was analyzed by fluorescence-activated cell sorter (FACS) analysis after 48 h. In each case, the limit dilution was reached to assess the amount of transductant retroviral vector particles. To assess the amount of viral particles produced, the RT activity (RT assay) was tested on the same serial dilutions. Ten microliters of culture supernatant was added to 50 μl of a reverse transcription mix {60 mM Tris-Cl (pH 8), 75 mM NaCl, 0.06% Nonidet P-40 substitute (Sigma), 0.7 mM $MnCl_2$, 6 mM dithiothreitol, 6 $\mu g \cdot ml^{-1}$ oligo(dT), 12 $\mu g \cdot ml^{-1}$ poly(rA), and 2 $\mu Ci \cdot ml^{-1}$ [α-^{32}P]dTTP (specific activity, 3,000 Ci/mmol)}. After 1 h of incubation at 37°C, 5 μl was loaded onto DEAE paper (DE-81; Whatman) and then rinsed with 2× SSC (0.3 M NaCl, 0.03 M sodium citrate [pH 5]). The radioactivity (β-rays) of the sample was recorded by a storage phosphorscreen (Molecular Dynamics), measured with a phosophorimager (Fuji), and quantified by using MultiGauge software (Fuji).

Immunofluorescence staining and confocal microscopy. Immunofluorescence staining and confocal microscopy imaging were performed as previously described (23). Briefly, 293T cells (grown on polylysine-coated coverslips) or NIH 3T3 cells (grown directly on glass coverslips) were transfected and, 24 h to 48 h hours later (as indicated in Results), fixed (3% paraformaldehyde in phosphate-buffered saline [PBS]), permeabilized (0.2% Triton), and stained (see above for the antibodies used). In the case of CFP and Myc detection (see Fig. 3), images were acquired by use of a TCS SP5 AOBS spectral confocal microscope with 405-nm and 561-nm laser diodes and an HCX Plan Apo 63× 1.2 W Corr oil objective, supplied with Leica LAS AF SP5 software. In the case of capsid detection (see Fig. 6), images were acquired on an Axioplan 2 Zeiss CLSM 510 confocal microscope with an Argon 488/458 Plan Apochromat 63× 1.4-numerical-aperture oil objective (supplied with LSM 510 software) in the case of capsid detection.

Electron microscopy. Transfected 293T cells expressing wild-type and mutant F-MuLV Gag-Pol were washed in PBS and then fixed in a buffer containing 4% paraformaldehyde and 1% glutaraldehyde in 0.1 M phosphate (pH 7.2) for 48 h. Cells were washed again, harvested, and postfixed with 1% osmium tetroxide for 1 h. Cells were dehydrated in a graded series of ethanol solutions, and the final cell pellets were embedded in Epon resin, which was allowed to polymerize for 48 h at 60°C. Ultrathin sections were cut with a Reichert (Heidelberg, Germany) ultramicrotome, collected on copper grids, and stained with 5% uranyl acetate and 5% lead citrate. The grids were then observed with a Jeol (Tokyo, Japan) 1010 XC electron microscope.

Membrane flotation assay. The membrane flotation assay protocol used was adapted from one described previously (38). For each experiment, 110 cm^2 of 293T cells was transfected (see above). Twenty-two hours after transfection, cells were kept at 20°C for 2 h to slow down intracellular trafficking. The supernatant was then harvested and treated as described above. Cells were washed in ice-cold PBS and then resuspended in 10 mM Tris-HCl containing 1 mM EDTA and Complete protease inhibitor cocktail (Roche). All subsequent stages were performed in a cold room. Postnuclear supernatants (PNSs) were obtained after Dounce homogenization of cell suspensions and low-speed centrifugation and were adjusted at 150 nM NaCl. One hundred eighty microliters of this PNS was then mixed with 820 μl of 75% (wt/vol) sucrose in TNE (25 mM Tris-HCl [pH 7.4], 4 mM EDTA, 150 mM NaCl) and placed into the bottom of a centrifuge tube. On top of this PNS-containing 62% (wt/vol) sucrose mixture, 2.3 ml of 50% (wt/vol) sucrose in TNE buffer and 0.9 ml of 10% (wt/vol) sucrose in TNE buffer were layered. The gradients were centrifuged at 35,000 rpm for 16 h at 4°C in a Beckman SW60Ti rotor. Eight fractions of 500 μl were collected from the top of the centrifuge tube for immunoblotting as described above. The sucrose per-

TABLE 1. K_d values obtained for interactions between MA and all PIP species in the presence or absence of PS[a]

PIP species	Mean K_d ± SD		Fold change
	No PS[b]	In the presence of PS[c]	
PI(3)P	42.1 ± 13.7	43.3 ± 8.5	1.0
PI(4)P	25.3 ± 0.5	20.9 ± 3.2	1.2[d]
PI(5)P	47.4 ± 5.4	32.8 ± 7.8	1.4[d]
$PI(3,4)P_2$	15.1 ± 0.9	30.0 ± 5.1	2[e]
$PI(3,5)P_2$	24.9 ± 6.7	36.0 ± 3.8	1.4[e]
$PI(4,5)P_2$	21.7 ± 1.3	5.4 ± 1.7	4.0[d]
$PI(3,4,5)P_3$	15.6 ± 1.6	NA	

[a] Also given is the variation in K_d with the PS addition, either a decrease (i.e., enhanced affinity) or increase (i.e., lower affinity). NA, not applicable.
[b] PC/PIP ratio of 95:5.
[c] PC/PS/PIP ratio of 75:20:5.
[d] Decrease.
[e] Increase.

centage after centrifugation was verified by refractometry to confirm that the discontinuity of the gradient was conserved.

RESULTS

The specific interactions of MuLV MA with the PIPs are enhanced for $PI(4,5)P_2$ in the presence of PS *in vitro*. We determined the K_d, expressed in terms of accessible acidic phospholipid, for the interaction of MoMuLV MA and LUVs. To this end, we performed quantitative cosedimentation assays with LUVs composed of PC and the phosphoinositides either in the presence or in the absence of PS. After ultracentrifugation, the supernatant and pellets were analyzed by SDS-PAGE followed by transfer onto membranes, staining, and subsequent image analysis. Typical images of membranes representing the pellets and the supernatants for LUVs of different compositions that had been cosedimented with MA (1 μM) are shown in Fig. 1A for increasing accessible lipid concentrations (from 15.6 to 1.5 mg/ml).

From these images, we determined the fraction of bound protein, which is represented in Fig. 1B as a function of the acidic lipid concentration. Fitting these curves according to equation 1 allowed us to obtain the K_d value between MA and the different LUVs. The K_d value corresponds to the lipid concentration at which one-half of the protein is bound to the LUVs.

In these experiments, the unspecific sedimentation of MuLV MA was very low (less than 20%), which indicates that no MuLV MA aggregates were formed. Of note, no affinity was detected between MA and PC, as expected (data not shown). Also, there was no interaction between MA and PC/PS LUV containing PS at 20% (data not shown) or even at 40% (Fig. 1A and B). This was rather unexpected, since it was previously reported that under the same conditions, unmyristoylated HIV-1 MA showed a strong affinity for PS (15, 62), which was confirmed in our study (Fig. 1B). In one study, no clear interaction was observed between PIPs and HIV-1 MA under equivalent experimental conditions (15). However, under different experimental conditions, i.e., with myristoylated HIV-1 Gag in the presence of reticulocyte lysate factors, another study reported an in vitro interaction between HIV-1 MA and $PI(4,5)P_2$ (14).

From Fig. 1B, it can be seen that the binding of MuLV MA to $PI(4,5)P_2$ LUVs increases when the concentration of LUVs is increased. Of note, $PI(4,5)P_2$ has a higher negative charge per molecule than PS (about −3 for $PI(4,5)P_2$ versus −1 for PS [30]), and thus, 5% of $PI(4,5)P_2$ is approximately equivalent to 15% of PS. As MuLV MA does not interact with PC or PS (even at 40%) but interacts with the phosphoinositides, we conclude that the interaction is more likely to be specific rather than exclusively electrostatic.

The fit of the experimental data using equation 1 leads to a K_d of 21.7 ± 1.37 μM for LUVs containing 5% $PI(4,5)P_2$ (Table 1 and Fig. 1D).

Similarly, we performed the same experiments with all PIPs, and we observed a clear interaction between MuLV MA and all of them (images not shown), which allowed us to determine the K_d for each phosphoinositide (Fig. 1C and Table 1). K_d values were calculated by considering only the concentration of accessible PIPs, as there was no interaction with PC/PS (60:40) LUVs. The K_d ranged from 15.1 ± 0.8 μM for $PI(3,4)P_2$ to 42.1 ± 13.7 μM for PI(3)P (lowest affinity). Some members of the PIP family showed higher affinities than others. For the monophosphorylated PIPs, the highest affinity (lower K_d) was observed for PI(4)P. In the case of polyphosphorylated PIPs, this tendency was conserved, as the only PIP lacking a phosphate at position 4 [$PI(3,5)P_2$] had the lowest affinity.

We also investigated whether the addition of both PS and PIPs potentiated the interaction with MA (Table 1 and Fig. 1D). The interaction of MA and PC/PS/$PI(4,5)P_2$ LUVs is higher than that for PC/$PI(4,5)P_2$ LUVs without PS, as the curve shown in Fig. 1B is shifted toward the left in the presence of PS. The fit of the experimental data using equation 1 leads to a K_d of 5.4 ± 1.7 μM for LUVs containing 20% PS and 5% $PI(4,5)P_2$, which represents approximately a fourfold-lower affinity than that without PS (Table 1 and Fig. 1D). In contrast, there was no significant decrease in the K_d upon the addition of PS together with the other PIPs (Fig. 1D and Table 1). Thus, the addition of PS to the LUV provided stereospecificity to the MA/$PI(4,5)P_2$ interactions.

Our results suggest that there is a difference between HIV-1 MA and MuLV MA in the way in which they bind PIPs. In our test, unmyristoylated MuLV MA binds to $PI(4,5)P_2$ but not HIV-MA, which binds to PS. For MuLV MA, the specificity of the interaction with $PI(4,5)P_2$ is increased by the presence of PS.

Mutations in the polybasic region of MuLV MA inhibit its interaction with $PI(4,5)P_2$ *in vitro*. The N-terminal MA domain of MuLV Gag contains a polybasic region that could play a role in Gag-cell membrane binding (36, 46, 52), as previously reported for several other retroviruses, notably HIV-1 and RSV (14). Phylogenetic sequence analysis reveals the presence of several basic residues and a conserved basic cluster located at the N terminus of MuLV MA domains from exogenous (MoMuLV and Friend MuLV) or endogenous (neuro-2a-associated retrovirus [NeRV]) strains. A previous study (52) showed that mutations in this basic region of MoMuLV MA impair virus production. As PIPs are acidic lipids, the polybasic $R_{31}KR\ R_{34}$ region of MA is likely to be involved in the interaction. We therefore introduced substitution mutations into the unmyristoylated recombinant MA protein (Fig. 2A), changing basic residues to either neutral (mutants m1 and m2)

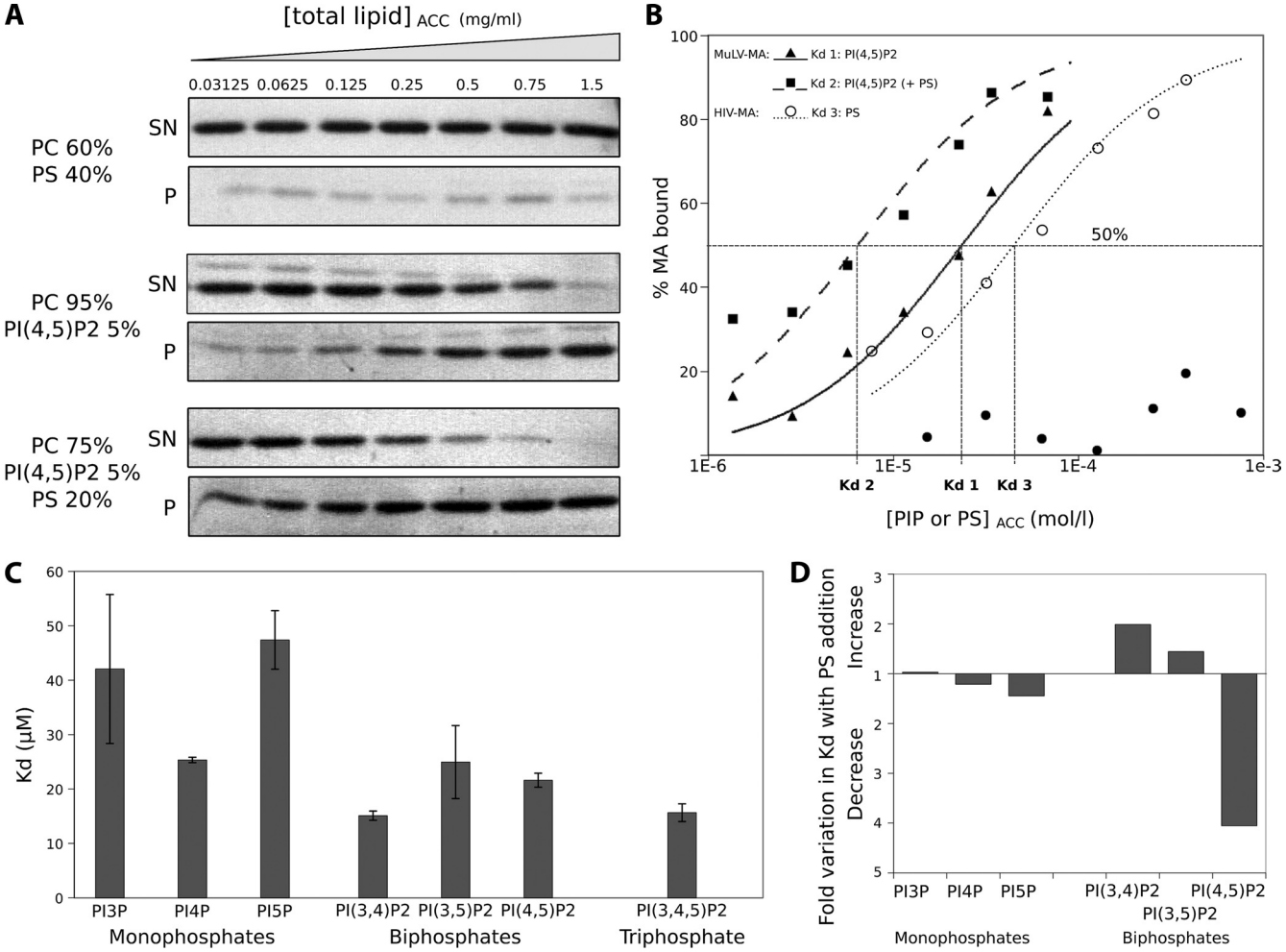

FIG. 1. Binding of recombinant MoMuLV MA to LUVs measured by a cosedimentation assay. Pellets (P) and supernatants (SN) were migrated on gels and then transferred onto membranes and stained with Coomassie blue for visualization and quantification. (A) Images of the membranes corresponding to the binding of MoMuLV MA to PC/PS (60:40) (top), 95% PC/PI(4,5)P_2 (95:5) (medium), and PC/PS/PI(4,5)P_2 (75:20:5) (bottom panels). (B) The percentages of MA bound are represented at different acid lipid compositions. The *x* axis is the accessible (ACC) PI(4,5)P_2 concentration. The curves are the least-square fits of equation 1 (see Materials and Methods), which yield the value for the molar partition coefficient, *K*, from which the affinity constant, K_d ($K_d = 1/K$), can be deduced. ●, MuLV MA nonfitted values (PS). (C) Graph summarizing the K_d values obtained by repeating the same experiments for all the phosphoinositides {data represent means ± standard deviations obtained from at least two independent measurement [four for PI(4,5)P_2]}. (D) Graph representing the variation in K_d calculated by comparing the K_d in the presence of PS (LUVs composed of PC/PS/PIP [75:20:5]) and in its absence (LUVs composed of PC/PIP [95:5]). Data were obtained in two independent experiments for PI(4,5)P_2 and one experiment for the other phosphoinositides.

or acidic (mutant m3) amino acids. Due to the low solubility of these mutants, the recombinant proteins (wild type and mutants) were purified under denaturing conditions (see Materials and Methods). Unfortunately, the m2 mutant aggregated and could not be analyzed. Under these conditions, the affinity of the wild-type MA protein for PC/PS/PI(4,5)P_2 (75:20:5) LUVs was similar to the result reported in Fig. 1 and gave a K_d of 7.6 ± 0.7 μM (Fig. 2B and C). In contrast, the m1 and m3 mutants showed no measurable affinity (less than 35% of protein bound even at the highest lipid concentrations) (Fig. 2C). In conclusion, our results showed that the polybasic region $R_{31}KR\ R_{34}$ in MA is required for the interaction of MuLV MA with PI(4,5)P_2/PS-containing membranes *in vitro*.

Overexpression of the 5ptaseIV enzyme causes a decrease in the level of MuLV production. To examine whether PI(4,5)P_2 is important for MuLV particle production in cells, we did experiments aimed at modifying the PI(4,5)P_2 pool in cells expressing Gag. The enzyme 5ptase IV is a phosphatase that specifically removes PIP phosphorylation at position 5, changing in particular PI(4,5)P_2 into PI(4)P [but also PI(3,4,5)P_3 into PI(3,4)P]. The activity of the enzyme was verified. We cotransfected 293T cells with pPH-PLC-CFP, which allows the expression of the CFP-coupled PH domain of the phospholipase C that specifically binds to PI(4,5)P_2, and a vector expressing either wild-type or mutant 5PtaseIV (or LacZ as a control). The plasma membrane localization of PH-phospholipase C was observed under conditions of LacZ or 5Ptase Δ1 overexpression (Fig. 3C, left and right, respectively). This membrane localization is completely lost under conditions of 5PtaseIV overexpression (Fig. 3C, middle), which suggests that the en-

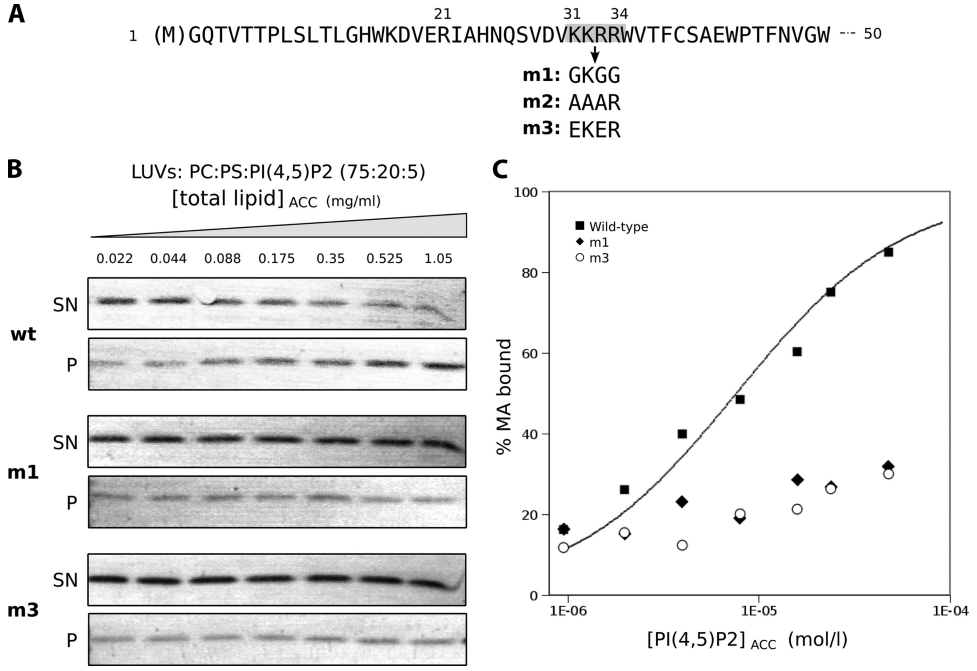

FIG. 2. Binding of recombinant MoMuLV MA mutants to LUVs measured by the cosedimentation assay. (A) Mutagenesis of MoMuLV MA basic residues. The first 50 amino acids (total MoMuLV MA consists of 131 residues) are shown. Mutations and clones' names are noted below the sequence. (B) Recombinant wild-type (wt) and mutant MA were subjected to cosedimentation assays as described in the legend of Fig. 1. Images of the membranes correspond to the binding of MoMuLV wild-type, m1, and m3 MA proteins to PC/PS/PI(4,5)P_2 (75:20:5) LUVs. Data for the m2 mutant are not shown, as it aggregated. SN, supernatant; P, pellet. (C) The percentage of MA bound is represented. The curve is the least-square fit of equation 1. The results shown here are representative of three independent experiments.

zyme is active in depleting PI(4,5)P_2 from the plasma membrane. We then overexpressed 5ptaseIV and MuLV Gag together in 293T cells and measured viral particle production by an RT test (Fig. 3A). The reference activity (100%) was measured in the presence of a reporter control gene, YFP. In the presence of wild-type 5PtaseIV, viral production was reduced by fivefold (20% ± 4% of the control), while in the presence of the 5PtaseIV Δ1 mutant, viral production was less affected (65% ± 8% of the control). By immunoblotting, we found that the overexpression 5ptaseIV caused a decrease in viral particle production (Fig. 3B, top) without a significant modification of the intracellular level of Gag (Fig. 3B, middle) or actin (Fig. 3B, bottom), while the 5ptaseIV Δ1 mutant had little effect on viral particle release. The results showed that decreasing the intracellular PI(4,5)P_2 pool partially inhibits viral production.

Mutations in the polybasic region of the Friend MuLV MA domain impair virus production. To further examine the role of the basic residues in Gag membrane binding and assembly in cells, we generated several mutants of the MA domain in a Friend MuLV Gag-Pol expression vector (pY1) (57) (Fig. 4A). Mutants were classified into two groups. The first group, already characterized in vitro, contained three mutants (m1, m2, and m3) of the polybasic region $R_{31}KRR_{34}$. In the m1 and m2 mutants, alanine or glycine residues were substituted for basic residues, while in m3, basic residues were changed to glutamic acid. The second group contained three mutants (m4, m5, and m6) of single arginine residues located in distant regions from the polybasic region (Fig. 4A).

To study the effects of the MA mutations on virus production and infectivity, we cotransfected 293T cells with plasmids expressing wild-type or mutant Gag-Pol and a murine envelope (Env) protein together with the packageable MuLV-enhanced GFP vector in order to produce retroviral vector particles that are able to achieve a single round of infection. This method allowed us to evaluate the production and the one-round replication of the MuLV retroviral vector. First, levels of Gag and Env proteins in the culture supernatant and in cell lysates were monitored 24 h posttransfection by immunoblotting using anti-capsid (CAp30) and anti-envelope (gp70) antibodies. All MA mutants allowed the synthesis of Pr65Gag (Fig. 4B, top), even though intracellular Gag levels and maturation profiles were slightly different from those of wild-type Gag, notably for mutants m1 and m3. The intracellular accumulation of Gag and Gag-derived products might be due either to a lower degradation or a higher production rate of Gag. Intracellular Env expression was equivalent for all the mutants in comparison with the wild type (Fig. 4B, top).

Only the MA mutants from the second group (m4, m5, and m6) were able to produce detectable amounts of retroviral vector particles similar to the wild-type level (Fig. 4C, bottom). These particles incorporated a normal amount of envelope protein. No particle production was detected for the m1 to m3 mutants, indicating that this MA region is essential for MuLV-based retroviral vector production.

Second, to verify if the particles produced were functional, we measured the RT activity of the cell culture supernatants and the single round of replication by transducing NIH 3T3 cells and by monitoring GFP expression by FACS analysis (Fig.

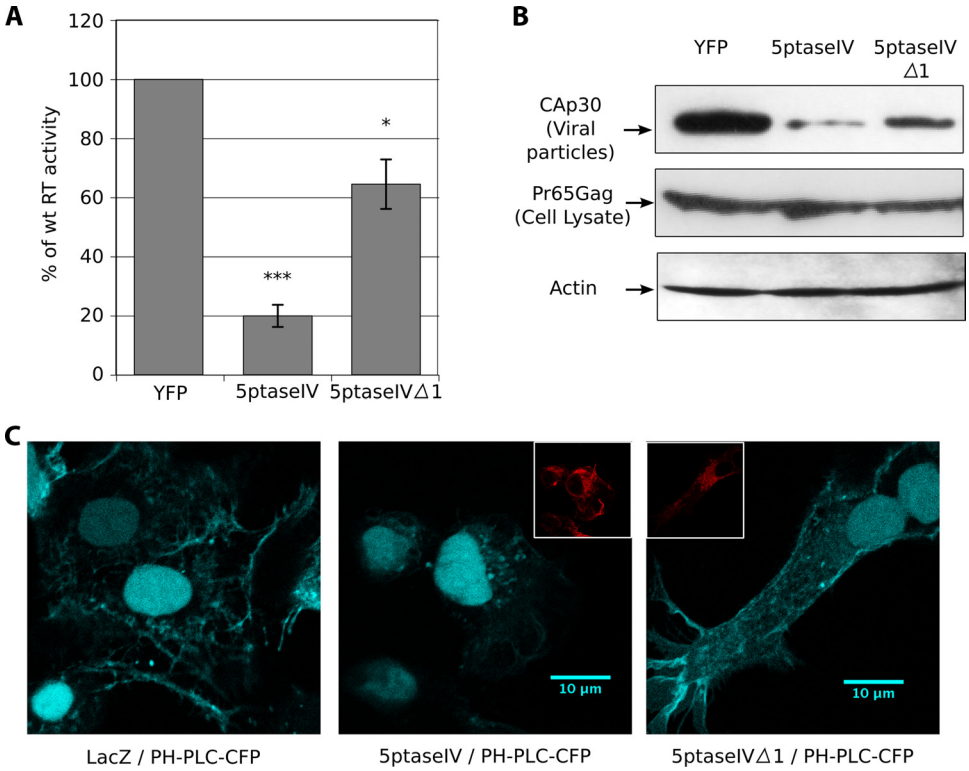

FIG. 3. Particle release upon coexpression with 5PtaseIV. 293T cells were transfected with pY1 (Gag-Pol expression) together with pCS2-Venus (YFP expression [control]), pcDNA 4/T0 5PtaseIV (5PtaseIV expression), or pcDNA 4/T0 5PtaseIV Δ1 (inactive 5PtaseIV expression [control]). Cultures were harvested 24 h after transfection. (A) RT activity of culture supernatants compared to pY1/pCS2-Venus (100%). The statistical significances of differences were calculated by an unpaired *t* test. ***, *P* value of <0.0001; *, *P* value of <0.01. (B) Analysis of viral (MuLV Gag) and cellular (actin) protein contents in cell lysates and viral CAp30 in particles issued from cell culture supernatants by Western blotting, as indicated. (C) 5PtaseIV activity control. 293T cells were transfected with pPH-PLC-CFP (PH domain of phospholipase C fused to CFP) together with pLacZ (LacZ expression [control]), pcDNA 4/T0 5PtaseIV (5PtaseIV expression), or pcDNA 4/T0 5PtaseIV Δ1 (inactive 5PtaseIV expression [control]). Cells were fixed 24 h after transfection, permeabilized, and stained with antibodies against myc and with an anti-mouse antibody coupled to Alexa546. the CFP signal is shown in cyan, while myc staining is represented in red when present (threefold-reduced images).

4C and see Materials and Methods for details). For the m1 and m3 mutants, only low RT activity (5.51% ± 2.54% and 6.77% ± 3.52% of the wild-type level, respectively) (Fig. 4C) and a low retroviral vector titer (4% ± 0.55% and 6.35% ± 1.98% of the wild-type level, respectively) (Fig. 4C) were monitored. The m2 mutant had no RT activity and was not infectious. The m4, m5, and m6 mutants (group 2) had no significant effect on RT activity, and vector-transducing titers were similar to the wild-type levels. We noted a good agreement between RT activity, vector titer, and CAp30 levels in the supernatants (Fig. 4), suggesting that the mutations did not cause further transducing defects in the vector particles produced.

Overall, these results showed that the polybasic $R_{31}KR\ R_{34}$ region of MA is necessary for MuLV viral particle production, while each of the isolated basic residues appears to be dispensable.

Mutations in the MA polybasic region decrease the ability of MuLV Gag to bind to cellular membranes. To assess the membrane binding ability of wild-type and mutated Gag proteins in cells, membrane flotation assays were performed on 293T cell extracts expressing wild-type Gag or either one of the mutant Gag proteins. Cells were harvested and lysed 24 h posttransfection, and the resulting PNS was loaded at the bottom of a discontinuous sucrose gradient that was submitted to equilibrium flotation centrifugation (see Materials and Methods). Fractions were collected and analyzed by Western blotting to detect MuLV Gag and cellular markers (Fig. 5). The top fractions, notably fractions 2 and 3, contained cell membrane-associated proteins (the lysosomal membrane protein Lamp2 was used as a control for a membrane binding protein), while the bottom fractions contained cytosolic proteins (the ribosomal S6 protein was used as a control) (Fig. 5A). The percentage of membrane-bound Gag was evaluated and is reported in Fig. 5B. For wild-type FrMuLV and MoMuLV Gag proteins, the majority of Gag was associated with membranes at the top of the gradient (almost 100% in fractions 2 and 3), while myr(−)Gag lost its membrane binding ability (almost 100% in fractions 7 and 8) (Fig. 5A). The polybasic-region mutants of Gag harbored a different phenotype: less than 50% of Gag remained associated with membranes (48% ± 9% for m1, 25% ± 6% for m2, and 46% ± 12% for m3), with the rest being cytosolic (group 1) (Fig. 5A and B). In contrast, the isolated basic-residue mutants harbored a wild-type-like membrane binding ability (group 2) (Fig. 5A and B) except that only 72% (±7%) of m6 Gag was associated with membranes.

These results show that the polybasic $R_{31}KR\ R_{34}$ region of

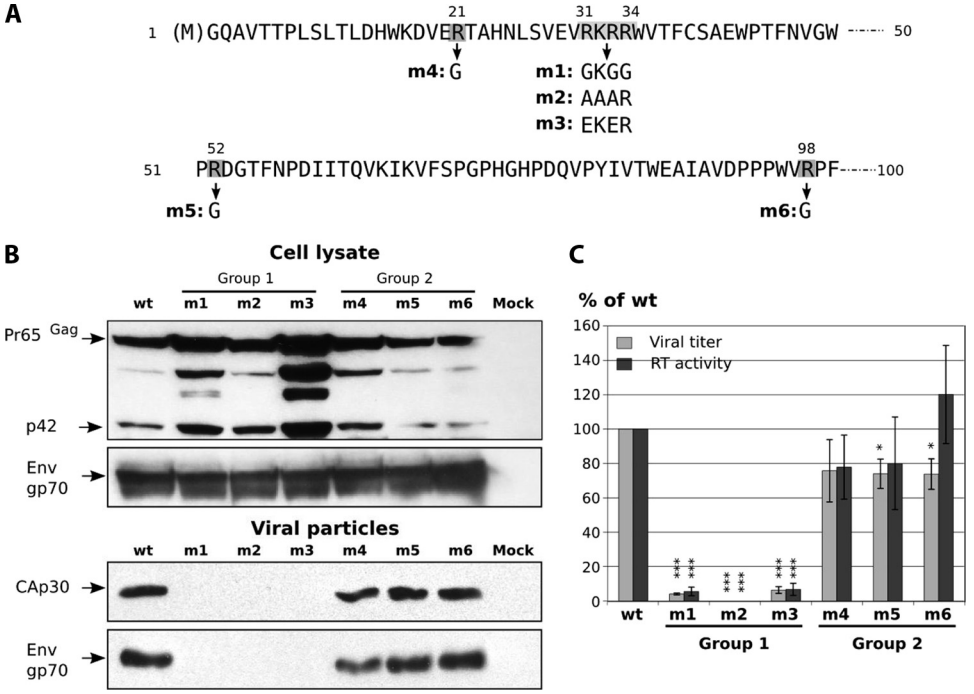

FIG. 4. Mutations in the matrix domain of Friend MuLV Gag. (A) Mutagenesis of Friend MuLV MA basic residues. The first 100 amino acids (total Friend MuLV MA consists of 131 residues) are shown. Mutations and clones' names are noted below the sequence. (B) Immunoblot analysis for the detection of the MuLV viral proteins Pr65 Gag, CAp30, and amphotropic Env (SUgp70) in cell lysates and in viral particles. (C) NIH 3T3 cells were infected with the wild-type (wt) MuLV vector or with either one of the six MA mutants and tested for GFP expression by FACS analysis 48 h after infection. The graph shows the viral titers and the RT activities of supernatants in comparison with those of wild-type Gag (100%; around 2.2×10^3 infectious particles per ml for wild-type viral titers). Mock supernatant was taken as the zero value for infectivity and RT activity measurements. Bars show mean values with standard deviations resulting from three independent experiments. Statistical significances of differences between the wild type and mutants were calculated by an unpaired *t* test. ***, *P* value of <0.0001; *, *P* value of <0.01.

MA is required for the stable membrane binding of MuLV Gag in cells.

Mutations in the polybasic region of MuLV MA result in intracellular Gag relocalization. Since mutations in the polybasic region of MA prevent virus production, the intracellular localization of the mutated Gag proteins was investigated by immunofluorescence microscopy in comparison with wild-type Gag. The study was performed by using both murine (NIH 3T3) and human (293T) cells, with the latter being used in order to avoid interference caused by the expression of endogenous MuLV Gag.

Figure 6 reports how MuLV Gag and mutated Gag proteins accumulated in NIH 3T3 murine cells. An unmyristoylated Gag-Pol mutant (44) was used as a control. As expected, wild-type Gag showed a punctate pattern, while myr(−)Gag was diffuse in the cytoplasm (Fig. 6). The m1, m2, and m3 mutants harbored phenotypes that were distinct from that of wild-type Gag. Mutant m1 was both diffuse and punctate in 88% of the cells (phenotype 1) (Fig. 6) and totally diffuse in 12% of them (phenotype 2). Mutant m2 was diffuse in the cytoplasm, with frequent patches observed only for NIH 3T3 cells (Fig. 6). Mutant m3 was both punctate and diffuse in all cells. The intracellular Gag localization for the single-basic-residue mutants (second group) was punctate in the cytoplasm, similarly to wild-type Gag (m4, m5, and m6) (Fig. 6). These observations suggest that the accumulation of large Gag oligomers in the cytoplasm is a prerequisite for viral particle production. Essentially similar results were obtained with 293T cells (data not shown).

Ultrastructure of MuLV mutant particles by electron microscopy. The ultrastructure and cellular localization of mutant Gag particles were analyzed by electron microscopy. Thin sections of cells expressing one mutant of each group (m3 for polybasic-region mutants and m6 for single-basic-residue mutants) were compared to wild-type Gag-Pol and myr(−)Gag-Pol. As expected, budding structures were observed mainly at the plasma membrane for wild-type Gag (Fig. 7A, right), and sometimes, particles were found in vesicles (intracellular compartments or plasma membrane diverticles) (Fig. 7A, left). Electron-dense assembled myr(−)Gag structures were found in the cytoplasm, without any apparent membrane (Fig. 7B). An intermediate phenotype was observed for the m3 mutant (polybasic-region mutant), since assembled particles were found in the cytoplasm, as for myr(−)Gag (Fig. 7C, left), or in intracellular compartments (Fig. 7C, middle and right), which could well correspond to virus-containing late endosomes or lysosomes in ultrathin sections (Fig. 7C, right). These observations were consistent with those obtained by confocal microscopy, as this Gag mutant appears either diffuse or punctate in the cytoplasm (m3) (Fig. 6). Moreover, m3 mutant Gag assembly did not take place at the plasma membrane (Fig. 7C), probably due to an improper trafficking of Gag and/or weak Gag-plasma membrane interactions (Fig. 2 *in vitro* and Fig. 5 *in cellulo*). Particles corresponding to the single-basic-residue m6

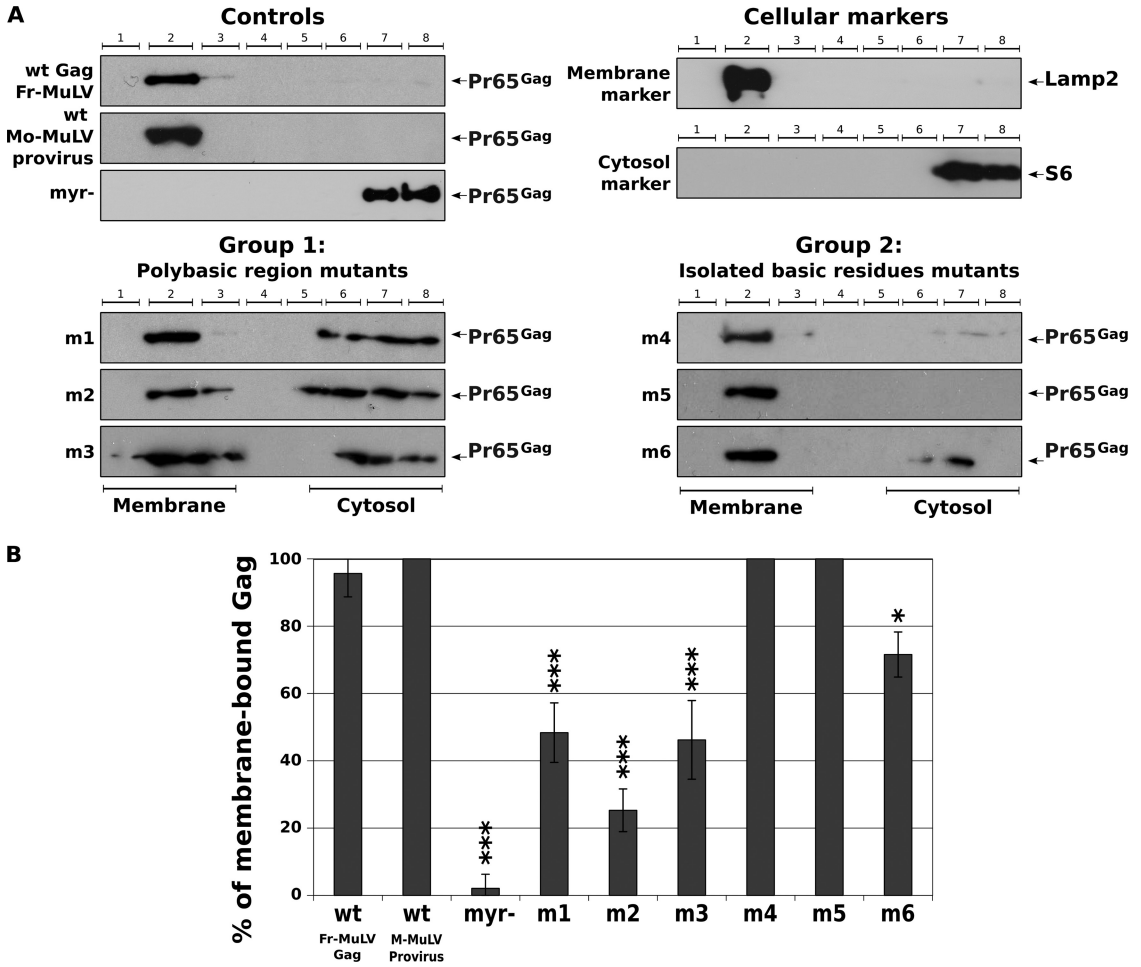

FIG. 5. Wild-type (wt) Gag and MA-mutated Gag membrane binding abilities. (A) 293T cells were transfected with either pRR88, pG2Amyr(−), pY1, or MA-mutated pY1 plasmids, as indicated, and 24 h posttransfection, the PNS was submitted to membrane flotation assays (see Materials and Methods). Cellular extracts were loaded at the bottom (fractions 6 to 8) of a discontinuous sucrose gradient. During centrifugation, membranes (and associated materials) float to the interface between 10% and 50% sucrose (fractions 2 and 3). The protein contents of the fractions were revealed by Western blotting, as indicated, for the cellular Lamp2 and S6 and for the viral Gag proteins. (B) The bands in A representative of membrane-bound or cytosolic Gag were scanned by densitometry and quantified by use of MultiGauge software. The percentage of membrane-bound Gag over total Gag (membrane-bound and cytosolic Gag) was calculated as indicated in the graph from data from at least three independent experiments. The significance of the differences observed was assessed by an unpaired *t* test. ***, *P* value of <0.0001; *, *P* value of <0.01. Fr-MuLV, Friend MuLV; M-MuLV, MoMuLV.

mutant bud at the plasma membrane and appeared to have a structure similar to that of the wild type (Fig. 7D).

This indicates that mutations of the MA polybasic region of MuLV Gag seem to prevent viral assembly and budding at the plasma membrane.

DISCUSSION

The aim of this study was to identify the viral and cellular determinants for MuLV Gag targeting to the plasma membrane. Two elements of the MA domain have historically been thought to be necessary for membrane anchoring: the myristic acid, which is required for Gag membrane binding and infectious-particle production (5, 22, 44, 52), and basic surface residues that could interact with phospholipid polar heads of the inner leaflet of the cell membrane (36). In the present study, the role of the basic residues of MuLV MA in Gag membrane binding, particle assembly, and release was examined. Two sets of mutants were designed, one group composed of three mutants in the conserved basic cluster (four basic residues in positions 31 to 34) and one group of three mutants with single substitutions of isolated basic residues exposed at the protein surface.

Our MA cosedimentation experiments with LUVs indicated that MuLV MA can interact with the biologically relevant PIP molecules [PI(4,5)P_2, PI(3)P, PI(4)P, PI(5)P, PI(3,4)P_2, PI(3,5)P_2, and PI(3,4,5)P_3] but not with PC (neutral) or with PS (acidic) alone (Fig. 1).

Under similar conditions, namely, using a nonmyristoylated MA protein with extruded LUVs in HEPES buffer, there is no specific interaction between HIV-1 MA and PIPs (15; data not shown). However, interactions between full-length HIV-1 Gag and PI(4,5)P_2 in a solution containing LUVs and reticulocyte lysate were noted previously (12). Several factors might ac-

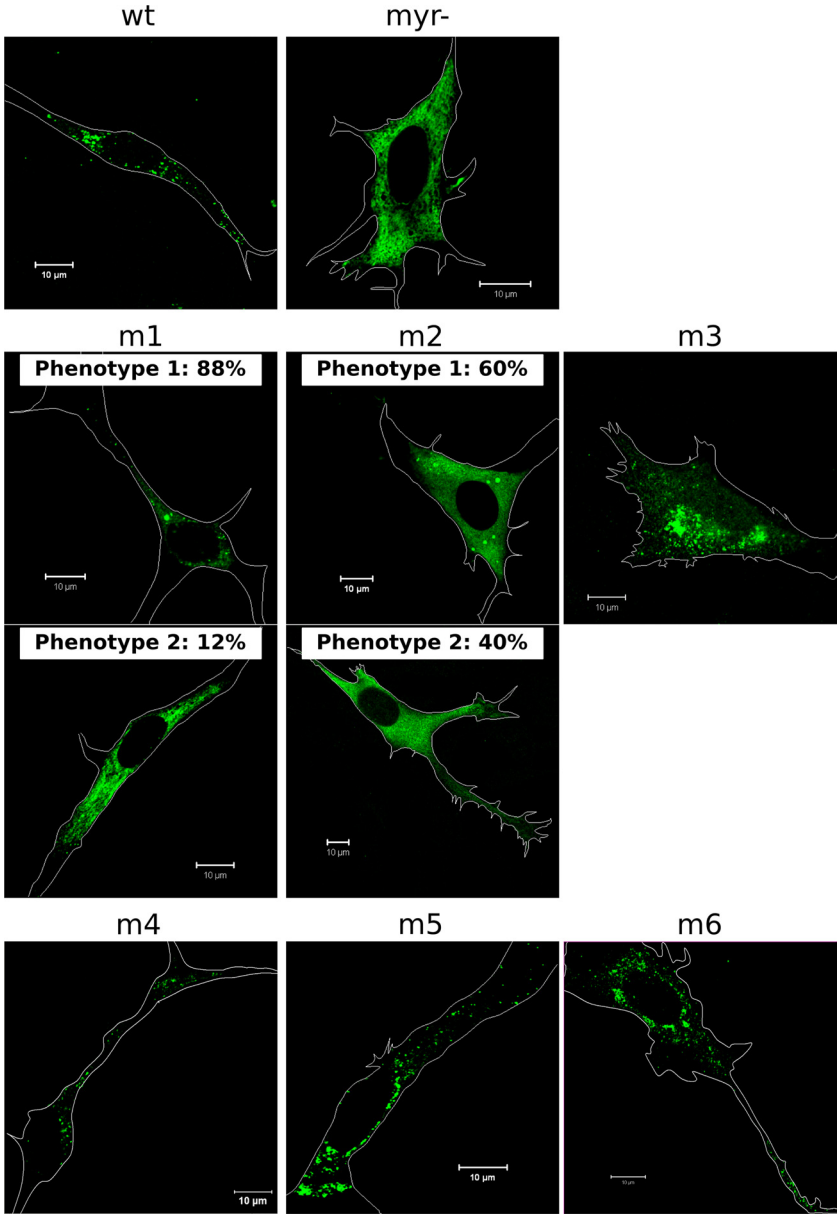

FIG. 6. Localization of wild-type and mutated Friend MuLV Gag in murine cells determined by immunoconfocal microscopy. NIH 3T3 cells were transfected with a Gag-Pol expression vector, either the wild type (wt) or harboring G2A myr(−) or MA mutations (m1 to m6, as indicated). Cells were fixed 48 h posttransfection, permeabilized, and stained with antibodies against CAp30 and with an anti-rabbit antibody coupled to Alexa488.

count for the different PIP binding properties of the MA proteins of MuLV and HIV-1. Thus, HIV-1 MA may need a cellular cofactor to bind PIPs, with this cofactor being present in the reticulocyte lysate. Our results indicate that the mechanism is different for MuLV MA. In fact, MuLV MA alone was able to specifically interact with LUVs containing PIPs in the absence of other cellular components (Fig. 1).

Unexpectedly, the affinity of $PI(4,5)P_2$ for MuLV MA increased dramatically (fourfold) upon the addition of PS (Fig. 1). In contrast, there was no such effect of PS on the other PIPs, suggesting that $PI(4,5)P_2$ is the major MA-interacting PIP in cells. In fact, all membrane layers containing $PI(4,5)P_2$ also contain PS, especially in the internal layer of the plasma membrane (32). A PS potentiation of the interaction between $PI(4,5)P_2$ and a cellular protein was also previously described for Myo1c, a protein of the myosin superfamily (26). The alternative mechanism, that is, an initial binding of PS but not of $PI(4,5)P_2$ alone and the stabilization of the interaction by $PI(4,5)P_2$, was also described for the protein kinase Cα (PKCα)-C2 domain (33). This cooperation between PS and PIPs appears to be a general feature for protein-membrane interactions. In the case of the PKCα-C2 domain, the binding of PS stabilizes the protein in an orientation that favors the interaction with $PI(4,5)P_2$. Similarly, in the case of MA, the

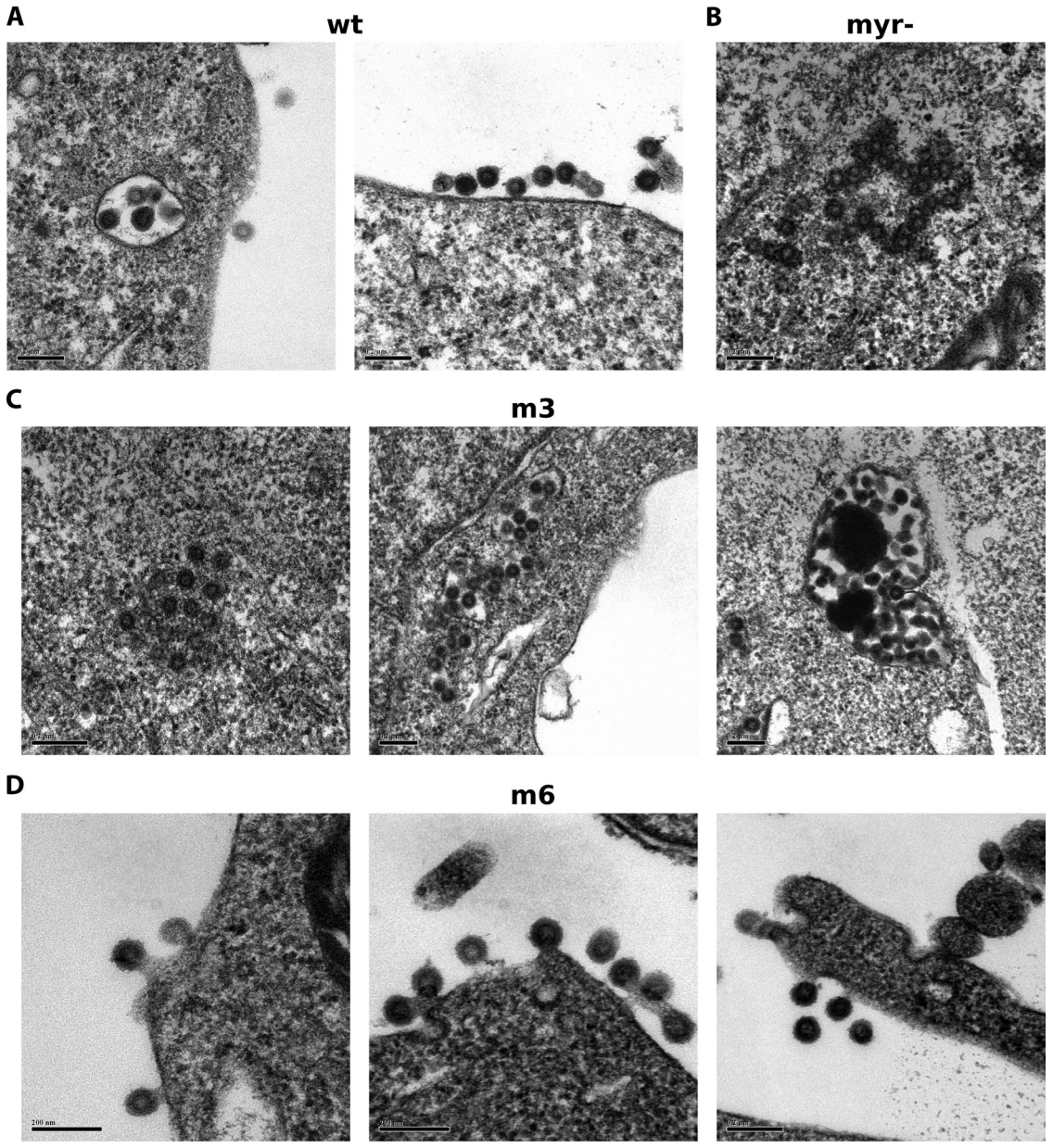

FIG. 7. Electron microscopy of wild-type and FrMuLV MA mutants. 293T cells transfected with Gag-Pol expression vectors were fixed in 4% paraformaldehyde–1% glutaraldehyde, treated, and observed as described in Materials and Methods. Wild-type (wt) MuLV Gag-Pol (A), G2A myr(−) (B), m3 (C), and m6 (D) are shown. Scale bars represent 200 nm.

interaction with PI(4,5)P_2 could trigger a conformational change or stabilize a specific orientation of the protein, allowing the interaction with PS. This model is supported by the fact that in other retroviruses, MA binding to PI(4,5)P_2 causes large structural modifications. Nuclear magnetic resonance data show that HIV-1 MA binding triggers the "myristyl switch" (48), and in vitro assembly data suggest that it may induce a profound reorganization in Gag oligomer formation (trimers instead of dimers) (1, 18). In the case of HIV-2, the first MA helix is destabilized upon PI(4,5)P_2 binding but is not sufficient to trigger the myristyl switch (49). EIAV MA also shows motions upon PI(4,5)P_2 binding, with possible consequences on trimerization (11). PI(4,5)P_2 binding could then be a key step in retroviral assembly, causing structural modifications that promote myristate exposure, multimerization, and PS binding.

The main difference between our results and previous observations of Myoc1 or PKCα-C2 is that for MuLV-MA, PS is providing the specificity for PI(4,5)P_2 binding.

The affinities of the interaction between MA and PI(4,5)P_2 alone for HIV-1, HIV-2, and EIAV were measured by nuclear magnetic resonance [with soluble species of truncated PI(4,5)P_2]. The K_d values were all quite high, between 100 and 300 μM (i.e., low affinities) (11, 48, 49). In the present study, the K_d was lower (K_d = 22.5 ± 1.3 μM), indicating a high affinity of the interaction between MuLV MA and PI(4,5)P_2.

This affinity may suggest the specific targeting and binding of MuLV Gag to the plasma membrane. In addition, the K_d obtained in the presence of PS, 5.4 ± 1.7 μM, enhances it. The affinity enhancement by PS may therefore also exist for other retroviruses. Another study was carried out on RSV matrix (16), but the authors reported no affinity of MA for PIPs. Those experiments, however, were done in a simpler system, and, as for HIV-1, the interaction with PIPs may necessitate more complex environments.

Highly consistent with our data, an analysis of retroviral particle lipidome was recently carried out (8). The authors showed that $PI(4,5)P_2$ and PS were the most enriched phospholipids in the particles for HIV-1 and MuLV, suggesting that these lipids are required for retrovirus assembly and most probably for Gag targeting and budding at the plasma membrane. A decrease in the level of viral production under conditions of 5PtaseIV overexpression was also reported, in agreement with our observations for MuLV Gag showing that the depletion of the intracellular $PI(4,5)P_2$ pool upon 5PtaseIV phosphatase overexpression decreased levels of MuLV release (Fig. 3).

Our data showed that the polybasic-region mutants partially lose the capacity to bind biomimetic membranes (Fig. 2) and cellular membranes (Fig. 5 and 6), indicating that the polybasic region $R_{31}KRR_{34}$ is involved in MuLV Gag membrane binding. The data also showed that multiple substitutions in this region impaired particle release and the localization of Gag (Fig. 4, 6, and 7), in agreement with previous work on MoMuLV Gag (52). Part of wild-type Gag traffics through the late endosomal/lysosomal pathway, as previously shown (3, 27, 51), while part of Gag is located at the plasma membrane (Fig. 7), but mutants were diffuse in the cytoplasm (Fig. 5 and 6) or eventually accumulated in intracellular compartments (Fig. 6 and 7), suggesting that the polybasic region of MuLV MA was not required for Gag targeting to internal compartments. By electron microscopy, the assembly of these mutants was observed either in the cytoplasm or in internal compartments, as opposed to wild-type Gag, which buds mainly at the plasma membrane (Fig. 7). This favors the notion that the MuLV MA basic cluster is most probably a signal for Gag targeting to and assembling at the plasma membrane. These results suggest that the polybasic region in MA not only is necessary for the stabilization of Gag membrane binding, in synergy with the anchoring of the myristate, but also contributes to the "choice" of the viral assembly site.

In contrast, the isolated basic-residue mutants harbored mostly wild-type-like phenotypes and have no major role in particle assembly.

We propose a scheme for MuLV Gag targeting and assembly, notably at the level of MA-cell membrane interactions. Our results favor the fact that MuLV Gag, having a high affinity for $PI(4,5)P_2$/PS, is directly addressed at the plasma membrane but could also bind endosomal membranes since MA is able to interact with all PIPs. The virions could then be produced by budding at the plasma membrane or at internal membranes, as suggested previously for HIV-1 (21, 23, 37, 41).

In conclusion, it appears that the MA-PIP interaction is an obligatory step for Gag membrane targeting and binding and, thus, for efficient retroviral assembly at the plasma membrane. Even though no classical PIP binding cleft has been observed for the MuLV MA domain, comparisons between several retroviral MA domains (36) allow the identification of a conserved polybasic region in the N-terminal domain of Gag. This MA basic cluster is most probably the PIP binding site of Gag and represents a potential target for new antiviral drug design.

ACKNOWLEDGMENTS

We acknowledge the PLATIM IFR128 microscope platform at ENS Lyon (France), Mike Spielt in the M. Summers laboratory for providing us the recombinant HIV-1 MA protein, E. Freed for providing us pcDNA4TOMyc5ptaseIV and the Δ1 mutant, W. Mothes for providing us plasmid pPH-PLC-CFP, and A. Rein for providing us the anti-CAp30 rabbit antibody. We gladly thank Jorge Vera for his helpful suggestions concerning the purification of MA proteins under denaturing conditions.

This work was supported by INSERM and CNRS (grant RISC AO 2008 to D.M.). We gratefully acknowledge partial support from the NIH (grant AI30917 to M.F.S.). E.H.-P. is a fellowship receiver of the French Government.

REFERENCES

1. **Alfadhli, A., R. L. Barklis, and E. Barklis.** 2009. HIV-1 matrix organizes as a hexamer of trimers on membranes containing phosphatidylinositol-(4,5)-bisphosphate. Virology **387:**466–472.
2. **Andrawiss, M., Y. Takeuchi, L. Hewlett, and M. Collins.** 2003. Murine leukemia virus particle assembly quantitated by fluorescence microscopy: role of Gag-Gag interactions and membrane association. J. Virol. **77:**11651–11660.
3. **Basyuk, E., T. Galli, M. Mougel, J. Blanchard, M. Sitbon, and E. Bertrand.** 2003. Retroviral genomic RNAs are transported to the plasma membrane by endosomal vesicles. Dev. Cell **5:**161–174.
4. **Blin, G., E. Margeat, K. Carvalho, C. A. Royer, C. Roy, and C. Picart.** 2008. Quantitative analysis of the binding of ezrin to large unilamellar vesicles containing phosphatidylinositol 4,5 bisphosphate. Biophys. J. **94:**1021–1033.

4a. **Bradford, M. M.** 1976. A rapid and sensitive method for the quantitation of microgram quantities of protein utilizing the principle of protein-dye binding. Anal. Biochem. **72:**248–254.

5. **Bryant, M., and L. Ratner.** 1990. Myristoylation-dependent replication and assembly of human immunodeficiency virus 1. Proc. Natl. Acad. Sci. U. S. A. **87:**523–527.
6. **Camus, G., C. Segura-Morales, D. Molle, S. Lopez-Vergès, C. Begon-Pescia, C. Cazevieille, P. Schu, E. Bertrand, C. Berlioz-Torrent, and E. Basyuk.** 2007. The clathrin adaptor complex AP-1 binds HIV-1 and MLV Gag and facilitates their budding. Mol. Biol. Cell **18:**3193–3203.
7. **Cantor, C., and P. Schimmel.** 1998. Biophysical chemistry. Freeman, New York, NY.
8. **Chan, R., P. D. Uchil, J. Jin, G. Shui, D. E. Ott, W. Mothes, and M. R. Wenk.** 2008. Retroviruses human immunodeficiency virus and murine leukemia virus are enriched in phosphoinositides. J. Virol. **82:**11228–11238.
9. **Chan, W., N. M. Sherer, P. D. Uchil, E. K. Novak, R. T. Swank, and W. Mothes.** 2008. Murine leukemia virus spreading in mice impaired in the biogenesis of secretory lysosomes and CA2+-regulated exocytosis. PLoS One **3:**e2713.
10. **Chen, B. K., I. Rousso, S. Shim, and P. S. Kim.** 2001. Efficient assembly of an HIV-1/MLV Gag-chimeric virus in murine cells. Proc. Natl. Acad. Sci. U. S. A. **98:**15239–15244.
11. **Chen, K., I. Bachtiar, G. Piszczek, F. Bouamr, C. Carter, and N. Tjandra.** 2008. Solution NMR characterizations of oligomerization and dynamics of equine infectious anemia virus matrix protein and its interaction with PIP2. Biochemistry **47:**1928–1937.
12. **Chukkapalli, V., I. B. Hogue, V. Boyko, W. Hu, and A. Ono.** 2008. Interaction between the human immunodeficiency virus type 1 Gag matrix domain and phosphatidylinositol-(4,5)-bisphosphate is essential for efficient Gag membrane binding. J. Virol. **82:**2405–2417.
13. **Coffin, J., S. Hughes, and H. Varmus.** 1997. Retroviruses. Cold Spring Harbor Laboratory Press, Cold Spring Harbor, NY.
14. **Conte, M. R., and S. Matthews.** 1998. Retroviral matrix proteins: a structural perspective. Virology **246:**191–198.
15. **Dalton, A. K., D. Ako-Adjei, P. S. Murray, D. Murray, and V. M. Vogt.** 2007. Electrostatic interactions drive membrane association of the human immunodeficiency virus type 1 Gag MA domain. J. Virol. **81:**6434–6445.
16. **Dalton, A. K., P. S. Murray, D. Murray, and V. M. Vogt.** 2005. Biochemical characterization of Rous sarcoma virus MA protein interaction with membranes. J. Virol. **79:**6227–6238.
17. **Darlix, J. L., M. Lapadat-Tapolsky, H. de Rocquigny, and B. P. Roques.** 1995. First glimpses at structure-function relationships of the nucleocapsid protein of retroviruses. J. Mol. Biol. **254:**523–537.

18. **Datta, S. A. K., Z. Zhao, P. K. Clark, S. Tarasov, J. N. Alexandratos, S. J. Campbell, M. Kvaratskhelia, J. Lebowitz, and A. Rein.** 2007. Interactions between HIV-1 Gag molecules in solution: an inositol phosphate-mediated switch. J. Mol. Biol. **365:**799–811.
19. **Di Paolo, G., and P. De Camilli.** 2006. Phosphoinositides in cell regulation and membrane dynamics. Nature **443:**651–657.
20. **Göttlinger, H. G., J. G. Sodroski, and W. A. Haseltine.** 1989. Role of capsid precursor processing and myristoylation in morphogenesis and infectivity of human immunodeficiency virus type 1. Proc. Natl. Acad. Sci. U. S. A. **86:** 5781–5785.
21. **Gousset, K., S. D. Ablan, L. V. Coren, A. Ono, F. Soheilian, K. Nagashima, D. E. Ott, and E. O. Freed.** 2008. Real-time visualization of HIV-1 Gag trafficking in infected macrophages. PLoS Pathog. **4:**e1000015.
22. **Granowitz, C., and S. P. Goff.** 1994. Substitution mutations affecting a small region of the Moloney murine leukemia virus MA Gag protein block assembly and release of virion particles. Virology **205:**336–344.
23. **Grigorov, B., F. Arcanger, P. Roingeard, J. Darlix, and D. Muriaux.** 2006. Assembly of infectious HIV-1 in human epithelial and T-lymphoblastic cell lines. J. Mol. Biol. **359:**848–862.
24. **Hansen, M., L. Jelinek, S. Whiting, and E. Barklis.** 1990. Transport and assembly of Gag proteins into Moloney murine leukemia virus. J. Virol. **64:**5306–5316.
25. **Hermida-Matsumoto, L., and M. D. Resh.** 1999. Human immunodeficiency virus type 1 protease triggers a myristoyl switch that modulates membrane binding of $pr55^{gag}$ and p17MA. J. Virol. **73:**1902–1908.
26. **Hokanson, D. E., J. M. Laakso, T. Lin, D. Sept, and E. M. Ostap.** 2006. Myo1c binds phosphoinositides through a putative pleckstrin homology domain. Mol. Biol. Cell **17:**4856–4865.
27. **Houzet, L., B. Gay, Z. Morichaud, L. Briant, and M. Mougel.** 2006. Intracellular assembly and budding of the murine leukemia virus in infected cells. Retrovirology **3:**12.
28. **Jin, J., N. M. Sherer, G. Heidecker, D. Derse, and W. Mothes.** 2009. Assembly of the murine leukemia virus is directed towards sites of cell-cell contact. PLoS Biol. **7:**e1000163.
29. **Krauss, M., and V. Haucke.** 2007. Phosphoinositides: regulators of membrane traffic and protein function. FEBS Lett. **581:**2105–2111.
30. **Krauss, M., and V. Haucke.** 2007. Phosphoinositide-metabolizing enzymes at the interface between membrane traffic and cell signalling. EMBO Rep. **8:**241–246.
31. **Leung, J., A. Yueh, F. S. K. J. Appah, B. Yuan, K. de los Santos, and S. P. Goff.** 2006. Interaction of Moloney murine leukemia virus matrix protein with IQGAP. EMBO J. **25:**2155–2166.
32. **Low, M. G., and J. B. Finean.** 1977. Modification of erythrocyte membranes by a purified phosphatidylinositol-specific phospholipase C (Staphylococcus aureus). Biochem. J. **162:**235–240.
33. **Manna, D., N. Bhardwaj, M. S. Vora, R. V. Stahelin, H. Lu, and W. Cho.** 2008. Differential roles of phosphatidylserine, PtdIns(4,5)P2, and PtdIns(3,4,5)P3 in plasma membrane targeting of C2 domains. Molecular dynamics simulation, membrane binding, and cell translocation studies of the PKCalpha C2 domain. J. Biol. Chem. **283:**26047–26058.
34. **Muriaux, D., J. L. Darlix, and A. Cimarelli.** 2004. Targeting the assembly of the human immunodeficiency virus type I. Curr. Pharm. Des. **10:**3725–3739.
35. **Muriaux, D., S. Costes, K. Nagashima, J. Mirro, E. Cho, S. Lockett, and A. Rein.** 2004. Role of murine leukemia virus nucleocapsid protein in virus assembly. J. Virol. **78:**12378–12385.
36. **Murray, P. S., Z. Li, J. Wang, C. L. Tang, B. Honig, and D. Murray.** 2005. Retroviral matrix domains share electrostatic homology: models for membrane binding function throughout the viral life cycle. Structure **13:**1521–1531.
37. **Ono, A., and E. O. Freed.** 2004. Cell-type-dependent targeting of human immunodeficiency virus type 1 assembly to the plasma membrane and the multivesicular body. J. Virol. **78:**1552–1563.
38. **Ono, A., and E. O. Freed.** 1999. Binding of human immunodeficiency virus type 1 Gag to membrane: role of the matrix amino terminus. J. Virol. **73:**4136–4144.
39. **Ono, A., S. D. Ablan, S. J. Lockett, K. Nagashima, and E. O. Freed.** 2004. Phosphatidylinositol (4,5) bisphosphate regulates HIV-1 Gag targeting to the plasma membrane. Proc. Natl. Acad. Sci. U. S. A. **101:**14889–14894.
40. **Paillart, J. C., and H. G. Göttlinger.** 1999. Opposing effects of human immunodeficiency virus type 1 matrix mutations support a myristyl switch model of Gag membrane targeting. J. Virol. **73:**2604–2612.
41. **Raposo, G., M. Moore, D. Innes, R. Leijendekker, A. Leigh-Brown, P. Benaroch, and H. Geuze.** 2002. Human macrophages accumulate HIV-1 particles in MHC II compartments. Traffic **3:**718–729.
42. **Reed, M., R. Mariani, L. Sheppard, K. Pekrun, N. R. Landau, and N. Soong.** 2002. Chimeric human immunodeficiency virus type 1 containing murine leukemia virus matrix assembles in murine cells. J. Virol. **76:**436–443.
43. **Rein, A.** 1994. Retroviral RNA packaging: a review. Arch. Virol. Suppl. **9:**513–522.
44. **Rein, A., M. R. McClure, N. R. Rice, R. B. Luftig, and A. M. Schultz.** 1986. Myristylation site in pr65gag is essential for virus particle formation by Moloney murine leukemia virus. Proc. Natl. Acad. Sci. U. S. A. **83:**7246–7250.
45. **Resh, M. D.** 2004. A myristoyl switch regulates membrane binding of HIV-1 Gag. Proc. Natl. Acad. Sci. U. S. A. **101:**417–418.
46. **Riffel, N., K. Harlos, O. Iourin, Z. Rao, A. Kingsman, D. Stuart, and E. Fry.** 2002. Atomic resolution structure of Moloney murine leukemia virus matrix protein and its relationship to other retroviral matrix proteins. Structure **10:**1627–1636.
47. **Saad, J. S., E. Loeliger, P. Luncsford, M. Liriano, J. Tai, A. Kim, J. Miller, A. Joshi, E. O. Freed, and M. F. Summers.** 2007. Point mutations in the HIV-1 matrix protein turn off the myristyl switch. J. Mol. Biol. **366:**574–585.
48. **Saad, J. S., J. Miller, J. Tai, A. Kim, R. H. Ghanam, and M. F. Summers.** 2006. Structural basis for targeting HIV-1 Gag proteins to the plasma membrane for virus assembly. Proc. Natl. Acad. Sci. U. S. A. **103:**11364–11369.
49. **Saad, J. S., S. D. Ablan, R. H. Ghanam, A. Kim, K. Andrews, K. Nagashima, F. Soheilian, E. O. Freed, and M. F. Summers.** 2008. Structure of the myristylated human immunodeficiency virus type 2 matrix protein and the role of phosphatidylinositol-(4,5)-bisphosphate in membrane targeting. J. Mol. Biol. **382:**434–447.
50. **Sandrin, V., D. Muriaux, J. Darlix, and F. Cosset.** 2004. Intracellular trafficking of Gag and Env proteins and their interactions modulate pseudotyping of retroviruses. J. Virol. **78:**7153–7164.
51. **Sherer, N. M., M. J. Lehmann, L. F. Jimenez-Soto, A. Ingmundson, S. M. Horner, G. Cicchetti, P. G. Allen, M. Pypaert, J. M. Cunningham, and W. Mothes.** 2003. Visualization of retroviral replication in living cells reveals budding into multivesicular bodies. Traffic **4:**785–801.
52. **Soneoka, Y., S. M. Kingsman, and A. J. Kingsman.** 1997. Mutagenesis analysis of the murine leukemia virus matrix protein: identification of regions important for membrane localization and intracellular transport. J. Virol. **71:**5549–5559.
53. **Spearman, P., R. Horton, L. Ratner, and I. Kuli-Zade.** 1997. Membrane binding of human immunodeficiency virus type 1 matrix protein in vivo supports a conformational myristyl switch mechanism. J. Virol. **71:**6582–6592.
54. **Suomalainen, M., K. Hultenby, and H. Garoff.** 1996. Targeting of Moloney murine leukemia virus Gag precursor to the site of virus budding. J. Cell Biol. **135:**1841–1852.
55. **Tang, C., E. Loeliger, P. Luncsford, I. Kinde, D. Beckett, and M. F. Summers.** 2004. Entropic switch regulates myristate exposure in the HIV-1 matrix protein. Proc. Natl. Acad. Sci. U. S. A. **101:**517–522.
56. **Wang, C. T., and E. Barklis.** 1993. Assembly, processing, and infectivity of human immunodeficiency virus type 1 Gag mutants. J. Virol. **67:**4264–4273.
57. **Yu, Q., and J. L. Darlix.** 1996. The zinc finger of nucleocapsid protein of Friend murine leukemia virus is critical for proviral DNA synthesis in vivo. J. Virol. **70:**5791–5798.
58. **Yu, Z., C. Beer, M. Koester, and M. Wirth.** 2006. Caveolin-1 interacts with the Gag precursor of murine leukaemia virus and modulates virus production. Virol. J. **3:**73.
59. **Yuan, B., X. Li, and S. P. Goff.** 1999. Mutations altering the Moloney murine leukemia virus p12 gag protein affect virion production and early events of the virus life cycle. EMBO J. **18:**4700–4710.
60. **Yuan, X., X. Yu, T. H. Lee, and M. Essex.** 1993. Mutations in the N-terminal region of human immunodeficiency virus type 1 matrix protein block intracellular transport of the Gag precursor. J. Virol. **67:**6387–6394.
61. **Zhou, W., and M. D. Resh.** 1996. Differential membrane binding of the human immunodeficiency virus type 1 matrix protein. J. Virol. **70:**8540–8548.
62. **Zhou, W., L. J. Parent, J. W. Wills, and M. D. Resh.** 1994. Identification of a membrane-binding domain within the amino-terminal region of human immunodeficiency virus type 1 Gag protein which interacts with acidic phospholipids. J. Virol. **68:**2556–2569.